MONTE CARLO CRITICALITY METHODS AND ANALYSIS CAPABILITIES IN SCALE

REACTOR SAFETY

KEYWORDS: *Monte Carlo, criticality safety, continuous energy and multigroup*

SEDAT GOLUOGLU,* LESTER M. PETRIE, JR., MICHAEL E. DUNN, DANIEL F. HOLLENBACH, and BRADLEY T. REARDEN

Oak Ridge National Laboratory, Nuclear Science and Technology Division
P.O. Box 2008, Building 5700, MS 6170, Oak Ridge, Tennessee 37831-6170

Received May 24, 2010
Accepted for Publication August 24, 2010

This paper describes the Monte Carlo codes KENO V.a and KENO-VI in SCALE that are primarily used to calculate multiplication factors and flux distributions of fissile systems. Both codes allow explicit geometric representation of the target systems and are used internationally for safety analyses involving fissile materials. KENO V.a has limiting geometric rules such as no intersections and no rotations. These limitations make KENO V.a execute very efficiently and run very fast. On the other hand, KENO-VI allows very complex geometric modeling. Both KENO codes can utilize either continuous-energy or multigroup cross-section data and have been thoroughly verified and validated with ENDF libraries through ENDF/B-VII.0, which has been first distributed with SCALE 6. Development of the Monte Carlo solution technique and solution methodology as applied in both KENO codes is explained in this paper. Available options and proper application of the options and techniques are also discussed. Finally, performance of the codes is demonstrated using published benchmark problems.

I. INTRODUCTION

The Monte Carlo codes KENO V.a and KENO-VI are used to calculate multiplication factors, flux distributions, fission densities, and other physics parameters of fissile systems. KENO V.a uses simple geometric bodies and arrays of units and holes to define the problem geometry and does not allow intersections. On the other hand, KENO-VI allows more complex geometric modeling by using both simple and complex geometric bodies and by allowing intersections and rotation of bodies in addition to arrays of units and holes. The added complexity allowed for in KENO-VI generally requires more computational time than the simplified geometry in KENO V.a.

Both KENO V.a and KENO-VI offer two cross-section modes: continuous energy and multigroup. Although it highly depends on the number of nuclides in each mixture, in general, the same problem using continuous-energy cross sections will run more slowly by a factor of 4 or more than when multigroup cross sections are used. However, continuous-energy cross sections offer more rigorous energy dependence treatment than multigroup cross sections. This may be very important for problems that exhibit variations in the cross sections resulting from physical distribution that cannot be represented using the limited one-dimensional (1-D) calculations used in processing multigroup cross sections.

Section II derives the transport equation used in both KENO codes for determining the steady-state particle distribution. Both continuous-energy and multigroup approaches are explained. Section III describes the actual random walk procedure used in KENO. Section IV explains the available options and features as well as the geometric capabilities of each version of KENO. Section V demonstrates code performance against experimental benchmark problems. Section VI summarizes the capabilities of the KENO codes.

Since the two codes are identical except for their respective geometry packages, from this point KENO will refer to both KENO V.a and KENO-VI, unless otherwise noted.

II. THE TRANSPORT EQUATION FOR MONTE CARLO SOLUTION IN KENO

The equation solved by KENO may be derived by starting with the time-dependent Boltzmann neutron transport equation, which may be written as

*E-mail: goluoglus@ornl.gov

$$\frac{1}{v}\frac{\partial\Phi}{\partial t}(\hat{X},E,\hat{\Omega},t)+\hat{\Omega}\cdot\nabla\Phi(\hat{X},E,\hat{\Omega},t)$$
$$+\Sigma_t(\hat{X},E,t)\Phi(\hat{X},E,\hat{\Omega},t)$$
$$=Q(\hat{X},E,\hat{\Omega},t)+\int_{E'}\int_{\Omega'}d\Omega'\,dE'$$
$$\times\Sigma_s(\hat{X},E'\rightarrow E,\hat{\Omega}'\rightarrow\hat{\Omega},t)\Phi(\hat{X},E,\hat{\Omega},t)\ ,\quad(1)$$

where

$\Phi(\hat{X},E,\hat{\Omega},t)$ = neutron flux ($\mathrm{n/cm^2\cdot s^{-1}}$) per unit energy at energy E per steradian about direction $\hat{\Omega}$ at position $\hat{X}$ at time t moving at speed v corresponding to E

$\Sigma_t(\hat{X},E,t)$ = macroscopic total cross section of the media ($\mathrm{cm^{-1}}$) at position $\hat{X}$, energy E, and time t

$\Sigma_s(\hat{X},E'\rightarrow E,\hat{\Omega}'\rightarrow\hat{\Omega},t)$ = macroscopic differential scattering cross section of the media ($\mathrm{cm^{-1}}$) at position $\hat{X}$, energy E', direction $\hat{\Omega}'$, and time t, for scattering to energy E and direction $\hat{\Omega}$ per unit energy and solid angle

$Q(\hat{X},E,\hat{\Omega},t)$ = volumetric source rate ($\mathrm{n/cm^3\cdot s^{-1}}$) at position $\hat{X}$ and time t per unit energy at energy E per steradian about direction $\hat{\Omega}$ (excludes scatter source).

Assuming there is no external source, the time-dependent equation can be converted to a stationary pseudocritical equation by introducing the multiplication factor k, which scales the fission source to exactly balance the loss rate:

$$\hat{\Omega}\cdot\nabla\Phi(\hat{X},E,\hat{\Omega})+\Sigma_t(\hat{X},E)\Phi(\hat{X},E,\hat{\Omega})=q(\hat{X},E,\hat{\Omega})\ .\quad(2)$$

Equation (2) is an eigenvalue problem with the total source defined as

$$q(\hat{X},E,\hat{\Omega})=\iint dE'\,d\Omega'\Phi(\hat{X},E',\hat{\Omega})$$
$$\times\Sigma_s(\hat{X},E'\rightarrow E,\hat{\Omega}'\rightarrow\hat{\Omega})$$
$$+\frac{1}{k}Q(\hat{X},E,\hat{\Omega})\ ,\quad(3)$$

where

k = largest eigenvalue of the homogeneous equation

$Q(\hat{X},E,\hat{\Omega})$ = fission source at position $\hat{X}$ for energy E and direction $\hat{\Omega}$ (all fission contributions to point E from all energy points in the previous generation).

This is the equation that is solved for both continuous-energy and multigroup modes by applying the Monte Carlo methodology.

II.A. Continuous-Energy-Mode Solution Methodology

Looking at travel from $\hat{X}$ to $\hat{X}'$ along direction $\hat{\Omega}$ with $\hat{X}'=\hat{X}+R'\hat{\Omega}$, where R' is the distance of travel along the direction $\hat{\Omega}$, Eq. (3) is rewritten

$$\frac{d}{dR'}\Phi(\hat{X}'-R'\hat{\Omega},E,\hat{\Omega})+\Sigma_t(\hat{X}'-R'\hat{\Omega},E)$$
$$\times\Phi(\hat{X}'-R'\hat{\Omega},E,\hat{\Omega})=q(\hat{X}'-R'\hat{\Omega},E,\hat{\Omega})\ .\quad(4)$$

Or, looking at travel from $\hat{X}'$ to $\hat{X}$,

$$-\frac{d}{dR}\Phi(\hat{X}-R\hat{\Omega},E,\hat{\Omega})+\Sigma_t(\hat{X}-R\hat{\Omega},E)$$
$$\times\Phi(\hat{X}-R\hat{\Omega},E,\hat{\Omega})=q(\hat{X}-R\hat{\Omega},E,\hat{\Omega})\ .\quad(5)$$

Now, an integrating factor is defined as follows:

$$e^{-T(R)}=e^{-\int_0^R\Sigma_t(\hat{X}-R'\hat{\Omega},E)dR'}\ ,$$

such that

$$\frac{d}{dR}e^{-\int_0^R\Sigma_t(\hat{X}-R'\hat{\Omega},E)\,dR'}$$
$$=-\Sigma_t(\hat{X}-R\hat{\Omega},E)e^{-\int_0^R\Sigma_t(\hat{X}-R'\hat{\Omega},E)\,dR'}\ .\quad(6)$$

Next, Eq. (5) is multiplied by the integrating factor:

$$-e^{-T(R)}\frac{d}{dR}\Phi(\hat{X}-R\hat{\Omega},E,\hat{\Omega})+e^{-T(R)}\Sigma_t(\hat{X}-R\hat{\Omega},E)$$
$$\times\Phi(\hat{X}-R\hat{\Omega},E,\hat{\Omega})=q(\hat{X}-R\hat{\Omega},E,\hat{\Omega})e^{-T(R)}\ .\quad(7)$$

After utilizing Eq. (6) in Eq. (7), we obtain

$$-\frac{d}{dR}\Phi(\hat{X}-R\hat{\Omega},E,\hat{\Omega})e^{-T(R)}$$
$$=q(\hat{X}-R\hat{\Omega},E,\hat{\Omega})e^{-T(R)}\ .\quad(8)$$

The resulting equation is integrated along the distance of travel R and rearranged (assuming R goes to infinity to include all space) as follows:

$$\Phi(\hat{X},E,\hat{\Omega}) = \int_0^\infty q(\hat{X}-R\hat{\Omega},E,\hat{\Omega})e^{-T(R)}\,dR \quad . \tag{9}$$

Assuming the fission neutrons to be isotropic, the fission source $Q(\hat{X},E,\hat{\Omega})$ can be written as

$$Q(\hat{X},E,\hat{\Omega}) = \frac{1}{4\pi}\int_{E'}\int_{\Omega'} dE'\,d\Omega'\Phi(\hat{X},E',\hat{\Omega}') \times \chi(\hat{X},E'\to E)\nu(\hat{X},E')\Sigma_f(\hat{X},E') \quad , \tag{10}$$

where

$\chi(\hat{X},E'\to E)$ = fraction of neutrons born at energy point E from fission at energy point E' in the media at position $\hat{X}$

$\nu(\hat{X},E')$ = number of neutrons resulting from a fission at energy point E' at position $\hat{X}$

$\Sigma_f(\hat{X},E')$ = macroscopic fission cross section of the material at position $\hat{X}$ for a neutron at energy point E'.

Substituting Eq. (3) into Eq. (9) yields Eq. (11):

$$\Phi(\hat{X},E,\hat{\Omega}) = \int_0^\infty d\,\mathrm{Re}^{-T(R)} \times \left\{\frac{1}{k}Q(\hat{X}-R\hat{\Omega},E,\hat{\Omega}) + \int_{E'}\int_{\Omega'} dE'\,d\hat{\Omega}'\,\Phi(\hat{X}-R\hat{\Omega},E',\hat{\Omega}')\Sigma_s(\hat{X}-R\hat{\Omega},E'\to E,\hat{\Omega}'\to\hat{\Omega})\right\} \quad . \tag{11}$$

Using Eq. (10), Eq. (11) can be written as

$$\Phi(X,E,\Omega) = \int_0^\infty d\,\mathrm{Re}^{-T(R)} \times \left\{\frac{1}{k}\frac{1}{4\pi}\int_{E'}\int_{\Omega'} dE'\,d\Omega'\,\nu(\hat{X}-R\hat{\Omega},E')\Sigma_f(\hat{X}-R\hat{\Omega},E')\chi(\hat{X}-R\hat{\Omega},E'\to E)\Phi(\hat{X}-R\hat{\Omega},E',\Omega') + \int_{E'}\int_{\Omega'} dE'\,d\Omega'\,\Phi(\hat{X}-R\hat{\Omega},E',\Omega')\Sigma_s(\hat{X}-R\hat{\Omega},E'\to E,\hat{\Omega}'\to\hat{\Omega})\right\} \quad . \tag{12}$$

The definition of k may be given as the ratio of the number of neutrons produced in the $(n+1)$'th generation to the number of neutrons produced in the n'th generation. Writing Eq. (12) in "generation notation," multiplying and dividing certain terms by $\Sigma_t(\hat{X},E)$, and multiplying both sides of the equation by $\nu(\hat{X},E)\Sigma_f(\hat{X},E)$ yields Eq. (13), which is solved by KENO in the continuous-energy mode:

$$\begin{aligned}\frac{\nu(\hat{X},E)\Sigma_f(\hat{X},E)}{\Sigma_t(\hat{X},E)}\Sigma_t(\hat{X},E)\Phi_n(\hat{X},E,\hat{\Omega}) &= \frac{\nu(\hat{X},E)\Sigma_f(\hat{X},E)}{\Sigma_t(\hat{X},E)}\Sigma_t(\hat{X},E)\left\{\frac{1}{k}\int_{E'}\int_{\Omega'} dE'\,\frac{d\hat{\Omega}'}{4\pi}\,\frac{\nu(\hat{X}-R\hat{\Omega},E')\Sigma_f(\hat{X}-R\hat{\Omega},E')}{\Sigma_t(\hat{X}-R\hat{\Omega},E')}\right.\\ &\quad\times\chi(\hat{X}-R\hat{\Omega},E'\to E)\Sigma_t(\hat{X}-R\hat{\Omega},E')\phi_{n-1}(\hat{X}-R\hat{\Omega},E'\hat{\Omega}')\\ &\quad+\int_{E'}\int_{\Omega'} dE'\,\frac{d\Omega'}{4\pi}\,\frac{\Sigma_s(\hat{X}-R\hat{\Omega},E'\to E,\hat{\Omega}'\to\hat{\Omega})}{\Sigma_t(\hat{X}-R\hat{\Omega},E')}\\ &\quad\left.\times\Sigma_t(\hat{X}-R\hat{\Omega},E')\Phi_n(\hat{X}-R\hat{\Omega},E',\hat{\Omega}')\right\} \quad .\end{aligned} \tag{13}$$

Note that on the left side of Eq. (13), $\nu(\hat{X},E)\Sigma_f(\hat{X},E)\Phi_n(\hat{X},E,\hat{\Omega})$ is the fission production for the n'th generation.

The solution strategy utilized by KENO solves Eq. (13) by using an iterative procedure. The fission production at point $\hat{X}$ at energy point E due to neutrons in the $(n-1)$'th generation, normalized to the system multiplication, is

$$\frac{1}{k}\int_{E'}\int_{\Omega'} dE' \frac{d\Omega'}{4\pi} \frac{\nu(\hat{X},E')\Sigma_f(\hat{X},E')}{\Sigma_t(\hat{X},E')} \chi(\hat{X},E' \rightarrow E)\Sigma_t(\hat{X},E')\Phi_{n-1}(\hat{X},E',\hat{\Omega}') \ . \tag{14}$$

The collision points used in KENO are chosen by selecting path lengths from the distribution $e^{-T(R)}$, which is the probability of transport from any position $\hat{X} - R\hat{\Omega}$ to position $\hat{X}$.

The collision density of neutrons at energy E per unit solid angle about $\hat{\Omega}$ resulting from the fission source produced by the $(n-1)$'th generation, normalized to the system multiplication, is

$$\Sigma_t(\hat{X},E)\int_0^\infty d\,\mathrm{Re}^{-T(R)} \left\{ \begin{array}{l} \frac{1}{k}\int_{E'}\int_{\Omega'} dE' \frac{d\Omega'}{4\pi} \frac{\nu(\hat{X}-R\hat{\Omega},E')\Sigma_f(\hat{X}-R\hat{\Omega},E')}{\Sigma_t(\hat{X}-R\hat{\Omega},E')} \\ \chi(\hat{X}-R\Omega,E' \rightarrow E)\Sigma_t(\hat{X}-R\hat{\Omega},E')\Phi_{n-1}(\hat{X}-R\hat{\Omega},E',\hat{\Omega}') \end{array} \right\} \ . \tag{15}$$

The scattering source at position $\hat{X}$ emerging at energy E and direction $\hat{\Omega}$ resulting from previous collisions in the same generation is

$$\int_{E'}\int_{\Omega'} dE'\, d\Omega' \frac{\Sigma_s(\hat{X},E' \rightarrow E,\hat{\Omega}' \rightarrow \hat{\Omega})}{\Sigma_t(\hat{X},E')} \times \Sigma_t(\hat{X},E')\Phi_n(\hat{X},E',\hat{\Omega}') \ .$$

The collision density from the scattering source at energy E, per solid angle about $\hat{\Omega}$, is

$$\Sigma_t(\hat{X},E)\int_0^\infty d\,\mathrm{Re}^{-T(R)}\int_{E'}\int_{\Omega'} dE'\, d\Omega' \times \frac{\Sigma_s(\hat{X}-R\hat{\Omega},E' \rightarrow E,\hat{\Omega}' \rightarrow \hat{\Omega})}{\Sigma_t(\hat{X}-R\hat{\Omega},E')} \times \Sigma_t(\hat{X}-R\hat{\Omega},E')\Phi_n(\hat{X}-R\hat{\Omega},E',\Omega') \ . \tag{16}$$

The total collision density, which is the sum of the collision densities from fission and scattering sources multiplied by $(\nu(\hat{X},E)\Sigma_f(\hat{X},E))/\Sigma_t(\hat{X},E)$, is the relationship from which KENO picks the source points for the next generation. The details of solving Eq. (16) will be discussed in Sec. III.

II.B. Multigroup-Mode Solution Methodology

Multigroup equations are derived in a manner similar to the continuous-energy equations. Converting Eq. (2) to multigroup form yields

$$\hat{\Omega}\cdot\nabla\Phi_g(\hat{X},\hat{\Omega}) + \Sigma_{tg}(\hat{X})\Phi(\hat{X},\hat{\Omega}) = q_g(\hat{X},\hat{\Omega}) \ , \tag{17}$$

where

g = energy group of interest

$\Phi_g(\hat{X},\hat{\Omega})$ = angular flux of neutrons having their energies in group g, at position $\hat{X}$ and angle $\hat{\Omega}$

$\Sigma_{tg}(\hat{X})$ = macroscopic total cross section of the media at position $\hat{X}$ for group g, corresponding to

$$\Sigma_{tg}(\hat{X}) = \frac{\int_{\Delta E}\int_{\Omega} dE\, d\Omega\, \Sigma_t(\hat{X},E)\Phi(\hat{X},E,\hat{\Omega})}{\int_{\Delta E}\int_{\Omega} dE\, d\Omega\, \Phi(\hat{X},E,\hat{\Omega})} \ ,$$

where

ΔE_g defines group g

$q_g(\hat{X},\hat{\Omega})q_g(X,\Omega)$ = total source contributing to energy group g at position $\hat{X}$ in direction $\hat{\Omega}$.

As in the continuous-energy-mode solution, using an integrating factor on both sides of Eq. (17) and defining

$$e^{T_g(R)} = e^{\int_0^R (\hat{X}-R'\hat{\Omega})dR'} \ ,$$

Eq. (18) can be written:

$$\Phi_g(\hat{X},\hat{\Omega}) = \int_0^\infty q_g(\hat{X}-R\hat{\Omega},\hat{\Omega})e^{-T_g(R)}\, dR \ . \tag{18}$$

At this point, since there is no external source, the problem becomes an eigenvalue problem with the total source defined as

$$q_g(\hat{X},\hat{\Omega}) = \sum_{g'}\int d\Omega'\, \Phi_{g'}(\hat{X},\hat{\Omega})\Sigma_s(\hat{X},g' \rightarrow g,\hat{\Omega}' \rightarrow \hat{\Omega}) + \frac{1}{k}Q_g(\hat{X},\hat{\Omega}) \ , \tag{19}$$

where

k = largest eigenvalue of the integral equation

$Q_g(\hat{X},\hat{\Omega})$ = fission source at position $\hat{X}$ for energy group g and direction $\hat{\Omega}$ (all fission contributions to group g from all energy groups in the previous generation)

$\Sigma_s(\hat{X},g' \rightarrow g,\hat{\Omega}' \rightarrow \hat{\Omega})$

= scattering cross section for scattering at position $\hat{X}$ from group g' and direction $\hat{\Omega}'$ to group g and direction $\hat{\Omega}$.

In terms of energy, the scatter can be defined as

$$\Sigma_s(X, g' \to g, \hat{\Omega}' \to \hat{\Omega}) = \frac{\displaystyle\int_{\Delta E_g}\int_{\Delta E_{g'}} \Sigma_s(\hat{X}, E' \to E, \hat{\Omega}' \to \hat{\Omega})\Phi(\hat{X}, E', \hat{\Omega}')\, dE'\, dE}{\displaystyle\int_{\Delta E_{g'}} \Phi(\hat{X}, E', \hat{\Omega}')\, dE'} \quad , \tag{20}$$

where

ΔE_g = energy-range-defining energy group g

$\Delta E_{g'}$ = energy-range-defining energy group g'.

Assuming the fission neutrons to be isotropic, the fission source $Q_g(\hat{X}, \hat{\Omega})$ can be written as

$$Q_g(\hat{X}, \hat{\Omega}) = \frac{1}{4\pi} \sum_{g'} \int_{\hat{\Omega}'} d\Omega'\, \Phi_{g'}(\hat{X}, \hat{\Omega}')\chi(\hat{X}, g' \to g)\nu_{g'}(\hat{X})\Sigma_{fg'}(\hat{X}) \quad , \tag{21}$$

where

$\chi(\hat{X}, g' \to g)$ = fraction of neutrons born in energy group g from fission in energy group g' in the media at position X

$\nu_{g'}(\hat{X})$ = number of neutrons resulting from a fission in group g' at position X

$\Sigma_{fg'}(\hat{X})$ = macroscopic fission cross section of the material at position $\hat{X}$ for a neutron in energy group g'.

Substituting Eq. (19) into Eq. (18) yields Eq. (22):

$$\Phi_g(\hat{X}, \hat{\Omega}) = \int_0^\infty d\,\mathrm{Re}^{-T_g(R)} \left\{ \frac{1}{k} Q_g(\hat{X} - R\hat{\Omega}, \hat{\Omega}) + \sum_{g'} \left[\int_{\Omega'} d\Omega'\, \Phi_{g'}(\hat{X} - R\hat{\Omega}, \hat{\Omega}')\Sigma_s(\hat{X} - R\hat{\Omega}, g' \to g, \hat{\Omega}' \to \hat{\Omega}) \right] \right\} \quad . \tag{22}$$

The definition of k may be given as the ratio of the number of neutrons in the $(n + 1)$'th generation to the number of neutrons in the n'th generation or the largest eigenvalue of the integral equation. Using Eq. (21), Eq. (22) can be written as

$$\Phi_g(\hat{X}, \hat{\Omega}) = \int_0^\infty d\,\mathrm{Re}^{-T_g(R)} \left\{ \frac{1}{k} \sum_{g'} \int_{\hat{\Omega}'} \frac{d\Omega'}{4\pi} \Phi_{g'}(\hat{X} - R\hat{\Omega}, \hat{\Omega}')\chi(\hat{X} - R\hat{\Omega}, g' \to g)\nu_{g'}(\hat{X})\Sigma_{fg'}(\hat{X} - R\hat{\Omega}) \right.$$
$$\left. + \sum_{g'} \left[\int_{\Omega'} d\Omega'\, \Phi_{g'}(\hat{X} - R\hat{\Omega}, \hat{\Omega}')\Sigma_s(\hat{X} - R\hat{\Omega}, g' \to g, \hat{\Omega}' \to \hat{\Omega}) \right] \right\} \quad . \tag{23}$$

Writing Eq. (23) in "generation notation," multiplying and dividing certain terms by $\Sigma_{tg}(\hat{X})$, and multiplying both sides of the equation by $\nu_g(\hat{X})\Sigma_{fg}(\hat{X})$ yields Eq. (24), which is solved by KENO in the multigroup mode:

$$\frac{\nu_g(\hat{X})\Sigma_{fg}(\hat{X})}{\Sigma_{tg}(\hat{X})} \Sigma_{tg}(\hat{X})\Phi_{g,n}(\hat{X}, \hat{\Omega})$$
$$= \frac{\nu_g(\hat{X})\Sigma_{fg}(\hat{X})}{\Sigma_{tg}(\hat{X})} \Sigma_{tg}(\hat{X}) \int_0^\infty d\,\mathrm{Re}^{-T_g(R)}$$
$$\times \left\{ \frac{1}{k} \sum_{g'} \int_{\Omega'} \frac{d\Omega'}{4\pi} \frac{\nu_g(\hat{X} - R\hat{\Omega})\Sigma_{fg'}(\hat{X} - R\hat{\Omega})}{\Sigma_{tg'}(\hat{X} - R\hat{\Omega})} \chi(\hat{X} - R\hat{\Omega}, g' \to g)\Sigma_{tg'}(\hat{X} - R\hat{\Omega})\Phi_{g',n}(\hat{X} - R\hat{\Omega}, \hat{\Omega}') \right\} \quad , \tag{24}$$

where

$$n = n\text{'th generation}$$

$$n - 1 = (n-1)\text{'th generation.}$$

Note that on the left side of Eq. (24), $\nu_g(X)\Sigma_{fg}(X)\Phi_{g,n}(X,\Omega)$ is the fission production for the n'th generation.

The solution strategy utilized by KENO in the multigroup mode solves Eq. (24) by using an iterative procedure. The fission production at point $\hat{X}$ in energy group g due to neutrons in the $(n-1)$'th generation, normalized to the system multiplication, is

$$\frac{1}{k}\sum_{g'}\int_{\Omega'}\frac{d\Omega'}{4\pi}\frac{\nu_{g'}(\hat{X})\Sigma_{fg'}(\hat{X})}{\Sigma_{tg'}(\hat{X})}\chi(\hat{X},g'\to g) \times \Sigma_{tg'}(\hat{X})\Phi_{g',n}(\hat{X},\hat{\Omega}') \ .$$

The collision points used in KENO are chosen by selecting path lengths from the distribution $e^{-T_g(R)}$, which is the probability of transport from any position $\hat{X}-R\hat{\Omega}$ to position $\hat{X}$.

The collision density of neutrons in group g per unit solid angle about $\hat{\Omega}$ resulting from the fission source produced by the $(n-1)$ generation, normalized to the system multiplication, is

$$\Sigma_{tg}(\hat{X})\int_0^\infty d\,\mathrm{Re}^{-T_g(R)} \times \left\{\begin{array}{l}\frac{1}{k}\sum_{g'}\int_{\Omega'}\frac{d\Omega'}{4\pi}\frac{\nu_{g'}(\hat{X}-R\hat{\Omega})\Sigma_{fg'}(\hat{X}-R\hat{\Omega})}{\Sigma_{tg'}(\hat{X}-R\hat{\Omega})} \\ \chi(\hat{X}-R\hat{\Omega},g'\to g)\Sigma_{tg'}(\hat{X}-R\hat{\Omega})\Phi_{g',n}(\hat{X}-R\hat{\Omega},\hat{\Omega}')\end{array}\right\} . \tag{25}$$

The scattering source at position $\hat{X}$ emerging in group g and direction $\hat{\Omega}$, resulting from previous collisions in the same generation, is

$$\sum_{g'}\int_{\Omega'}d\Omega'\frac{\Sigma_s(\hat{X},g'\to g,\hat{\Omega}'\to\hat{\Omega})}{\Sigma_{tg'}(\hat{X})} \times \Sigma_{tg'}(\hat{X})\Phi_{g',n}(\hat{X},\hat{\Omega}') \ .$$

The collision density from the scattering source in group g, per solid angle about $\hat{\Omega}$, is

$$\Sigma_{tg}(\hat{X})\int_0^\infty d\,\mathrm{Re}^{-T_g(R)}\sum_{g'}\int_{\Omega'}d\Omega' \times \frac{\Sigma_s(\hat{X}-R\hat{\Omega},g'\to g,\hat{\Omega}'\to\hat{\Omega})}{\Sigma_{tg'}(\hat{X}-R\hat{\Omega})} \times \Sigma_{tg'}(\hat{X}-R\hat{\Omega})\Phi g_{g',n}(\hat{X}-R\hat{\Omega},\hat{\Omega}') \ . \tag{26}$$

The total collision density, which is the sum of the collision densities from fission and scattering sources, times $(\nu_{g'}(\hat{X})\Sigma_{fg'}(\hat{X}))/\Sigma_{tg'}(\hat{X})$ is the relationship from which KENO picks the source points for the next generation. The details of solving Eq. (26) will be discussed in Sec. III.

III. THE SOLUTION ALGORITHM

KENO solves Eq. (16) in the continuous-energy mode and Eq. (26) in the multigroup mode. Because the Monte Carlo method is employed in the solution of Eqs. (16) and (26), every calculated quantity has a statistical uncertainty associated with it.

In order to minimize the statistical variation of k_{eff} and other calculated parameters per unit computer time, KENO utilizes weighted tracking, also known as implicit capture, rather than analog tracking. Weighted tracking accounts for absorption by reducing the neutron weight, rather than allowing the neutron history to be terminated by absorption. The details of this and other techniques used in treating collisions are discussed in Sec. III.D.

III.A. Problem Initialization

Based on the calculation mode selected, various initialization tasks are performed. In both modes, total cross sections for each mixture are determined from the nuclides provided in the mixing table. Each nuclide in the continuous-energy cross-section library has a union energy mesh that contains all the points from all reaction types. The points for each reaction type are selected such that they can re-create the continuous-energy cross sections within some tolerance, assuming a linear relation between adjacent points. Most reactions for a nuclide do not use the entire union mesh but are represented using energy points that are a subset of the union mesh. KENO will read all reaction cross sections for each nuclide at problem execution and map all reactions of that nuclide to the union mesh of the nuclide. This method allows the cross-section library to store only one energy mesh and allows faster sampling of the reactions during execution.

After the data initialization tasks are complete, the Monte Carlo random walk can be performed according to the procedures that are documented in Secs. III.B through III.K.

III.B. Initial Source Distribution

Before the Monte Carlo simulation can be performed, the initial source distribution of neutrons must be sampled. Each mixture is checked for the presence of fissionable material. For each fissionable mixture, the volume fraction of fissionable material must be calculated on a per nuclide basis to determine which fission energy distribution is used for each source neutron.

The first source distribution comprises the initial spatial coordinates, direction cosines, and energy for each neutron within the problem. The energy of each source neutron is sampled from the fission energy distribution of a fission reaction with a fissionable nuclide within the mixture. If more than one fissionable nuclide is present, the i'th nuclide is selected using the following relation:

$$\sum_{j=1}^{i-1} \Sigma_f^j < R \sum_{j=1}^{N} \Sigma_f^j \leq \sum_{j=1}^{i} \Sigma_f^j \ , \tag{27}$$

where

Σ_f^j = macroscopic fission cross section for the j'th nuclide

R = random number (0, 1]

N = total number of fissionable nuclides in the mixture.

Note that the relation in Eq. (27) requires the knowledge of the fission cross section at a particular energy. Therefore, an initial energy of 0.025 eV is assumed for selecting the appropriate nuclide to sample. If the fission cross sections of all fissionable nuclides of the mixture are zero at 0.025 eV, then the sampling energy is increased to the energy corresponding to the first nonzero fission cross section. Once the i'th nuclide is selected, the fission reaction of that nuclide at the initial energy of 0.025 eV is sampled, and the exit energy and angle after the sampled fission reaction are stored as the starting energy and angle of that neutron. In the multigroup mode, the energy of each source neutron is sampled from the multigroup fission spectrum $\chi(\hat{X}, g)$ of the mixture. Each initial neutron is assigned a default weight of $C \times WTAVG$, where C is the normalization factor determined as

$$C(ki, fc, \hat{\Omega}, E) = \sum_{E'} \frac{P(ki, fc, E', \hat{\Omega}, E)}{WTAVG(g', ki)} \ , \tag{28}$$

where

P = probability density function (pdf) for fission

ki = importance determined by the BIAS ID of the region (default = 1) and therefore is implicitly a function of spatial position

fc = index for first-chance fission, second-chance fission, etc., probabilities; fission probabilities are discussed in Sec. III.E

$WTAVG$ = default or user-specified average weight (Sec. III.D).

Since weights are defined in terms of energy groups, g' is the energy group corresponding to the exit neutron energy E'. In the multigroup mode, since all fission sources are isotropic, C is determined as

$$C(ki) = \sum_{g'} \frac{\chi(ki, g')}{WTAVG(g', ki)} \ . \tag{29}$$

As evidenced by Eqs. (28) and (29), normalization is determined based on the initial assigned weights. Note that since both P and χ sum to 1.0, if the average weights are constant with a value of 0.5, the normalization factors will be 2.0.

For the spatial distribution of initial neutrons, KENO offers various options under "START DATA." These start options are listed in Table I. The default start option, which is flat across the global array or unit, is usually sufficient. If the global array or unit has large outer dimensions with only a small fraction of the volume containing fissionable material, much time may be wasted in sampling positions that do not contain any fissionable material. If the fraction of the volume containing fissile material is relatively small, execution may terminate due to excessive time spent in sampling the source neutron distribution. Generally, this type of problem will run at a reasonable time once a good starting distribution is created. Changing the initial distribution is trivial and usually involves specifying a tightly fitting cuboid around the fissionable material.

III.C. Collision Site Selection

Since weighted tracking is employed, each neutron must be tracked until the history is terminated via leakage from the system or the particle weight drops sufficiently and it is "killed" via roulette. Given a homogeneous material, a neutron will travel, on average, 1 mean free path between collisons. The determination of the distance to the next collision is determined using the following pdf:

$$f(x)\, dx = \Sigma_t^m(E) e^{-\Sigma_t^m(E)x}\, dx \ , \tag{30}$$

where

$\Sigma_t^m(E)$ = macroscopic total cross section for mixture m at energy E

x = distance to the next collision.

The pdf in Eq. (30) describes the probability that a neutron will have an interaction between x and $x + dx$ along its flight path. Integrating Eq. (30) over the distance variable yields the following cumulative distribution function (cdf):

$$F(x) = \int_0^x dx'\, \Sigma_t^m(E) e^{-\Sigma_t^m(E)x'} = 1 - e^{-\Sigma_t^m(E)x} \ . \tag{31}$$

The next collision site is determined by setting the cdf in Eq. (31) equal to a random number R, uniformly distributed on the interval [0, 1) and solving for x:

TABLE I

Starting Distributions Available in KENO

Start Type	Starting Distribution
0	Uniform throughout fissile material within the volume defined by (a) the outer region of a single unit, (b) the outer region of a reflected array having the reflector key set true, (c) the boundary of the global array, or (d) a user-specified cuboid.
1	The starting points are chosen according to a cosine distribution throughout the volume of a user-specified cuboid. Points that are not in fissile material are discarded.
2	An arbitrary fraction of neutrons is started uniformly in the unit located at a user-specified position in the global array. The remainder of the neutrons is started in fissile material, from points chosen from a cosine distribution throughout the volume of a user-specified cuboid.
3	All neutrons are started at a user-specified position within the unit located at a user-specified position in the global array.
4	All neutrons are started at a user-specified position within user-specified units in the global array.
5	Neutrons are started uniformly in fissile material in user-specified units in the global array.
6	The starting distribution is arbitrarily input. The final neutron number to be started at a user-specified point relative to the global coordinate system or at a user-specified point relative to the unit located at a global array position is specified.
7	The starting points are chosen according to a flat distribution in the *X* and *Y* dimensions and a $[1.0 - \cos(z)]^2$ distribution in the *Z* dimension throughout the volume of a user-specified cuboid defined. Points that are not in fissile material are discarded.
8	Neutrons are started with flat distribution in *X* and *Y*, and a segmented distribution in *Z*, with user-specified *X*-*Y* limits and a user-specified relative fraction in *Z*.

$$R' = 1 - e^{-\Sigma_t^m(E)x} \quad , \quad R' \in [0,1)$$

$$1 - R' = e^{-\Sigma_t^m(E)x}$$

$$-\ln(1 - R') = \Sigma_t^m(E)x \quad , \quad R' \in [0,1)$$

$$x = -\ln(1 - R')/\Sigma_t^m(E) \quad . \tag{32}$$

Recognizing that $(1 - R)$ is also a uniformly distributed random number, albeit in the domain (0,1], we may rewrite Eq. (32) as

$$x = -\ln(R)/\Sigma_t^m(E) \quad . \tag{33}$$

Note that Eq. (31) requires the total cross section for mixture *m* at energy *E* in order to calculate the next collision site. If the neutron energy is in the unresolved resonance range (URR) of any of the nuclides in the mixture, and those nuclides have corresponding probability-table data, KENO samples the appropriate probability tables and recalculates the mixture total cross section at the neutron energy during the random walk. Details of the probability-table treatment are discussed in Sec. III.K. Once the revised $\Sigma_t^m(E)$ is determined, Eq. (33) is used to select the next collision site within mixture *m* at energy *E*. In the multigroup mode, there is no probability table, and the equation used to sample the next collision site is

$$x = -\ln(R)/\Sigma_{tg}^m \quad . \tag{34}$$

III.D. Collision Treatment

Once the collision site is determined, the collision can be modeled, and the postcollision parameters can be calculated. In the continuous-energy mode, each collision is modeled with an individual nuclide, whereas in the multigroup mode, no such distinction is made. If a mixture is defined by multiple nuclides, the target nuclide must be selected at each collision site. If there are *N* different nuclides present in a mixture, Eq. (35) can be used to select the *i*'th target nuclide for interaction:

$$\sum_{j=1}^{i-1} \Sigma_t^j(E) < R \sum_{j=1}^{N} \Sigma_t^j(E) \le \sum_{j=1}^{i} \Sigma_t^j(E) \quad , \tag{35}$$

where Σ_t^j is the macroscopic total cross section for the *j*'th nuclide at energy *E*.

As noted above, the collision energy may be in the URR of one or more nuclides within the mixture. Consequently, the total cross section for each nuclide that has

unresolved resonance data is sampled from the probability-table information prior to selecting the next collision site, as discussed in Secs. III.C and III.K. Subsequently, the sampled values for the total and partial reactions are stored for retrieval for determining the next collision type. Therefore, the macroscopic nuclide total cross-section values $\Sigma_t^j(E)$ that are used in Eq. (35) are those that are used to determine $\Sigma_t^m(E)$ in Eq. (33). With the corrected values for $\Sigma_t^j(E)$, Eq. (35) is used to select the target nuclide for interaction. In the multigroup mode, the calculation proceeds without having to choose a target nuclide since that information is not needed.

Because an explicit collision treatment is dictated by the continuous-energy cross-section data, the type of reaction must be modeled explicitly in the continuous-energy mode. Figure 1 provides a summary of the cross-section hierarchy and can be used as an aid to understanding the collision treatment in KENO in the continuous-energy mode.

After selecting the collision target, the absorption (absorbed), fission, $(n,2n)$, and $(n,3n)$ weights are determined. In the multigroup mode, $(n,2n)$ and $(n,3n)$ weights are not determined because corresponding reaction probabilities are not available. Subsequently, the neutron's weight is reduced by the nonabsorption probability:

$$w = \frac{\sigma_s^i(E)}{\sigma_t^i(E)} w_b = P_{nabs}(E) w_b \ , \tag{36}$$

where

$\sigma_s^i(E)$ = microscopic scattering cross section for the i'th (selected) nuclide at energy E

$\sigma_t^i(E)$ = microscopic total cross section for the i'th (selected) nuclide at energy E

$P_{nabs}(E)$ = nonabsorption probability of the neutron at energy E

w_b = weight before collision.

The absorption and fission weights are calculated using, respectively, the relations in Eqs. (37) and (38):

$$w_a = \frac{\sigma_a^i(E)}{\sigma_t^i(E)} w_b = P_{abs}(E) w_b \ , \tag{37}$$

where

$\sigma_a^i(E)$ = microscopic absorption cross section for the i'th (selected) nuclide at energy E

$P_{abs}(E)$ = absorption probability of the neutron at energy E

and

$$w_f = \frac{\bar{\nu}^i(E)\sigma_f^i(E)}{\sigma_t^i} w_b = P_{fiss}(E) w_b \ , \tag{38}$$

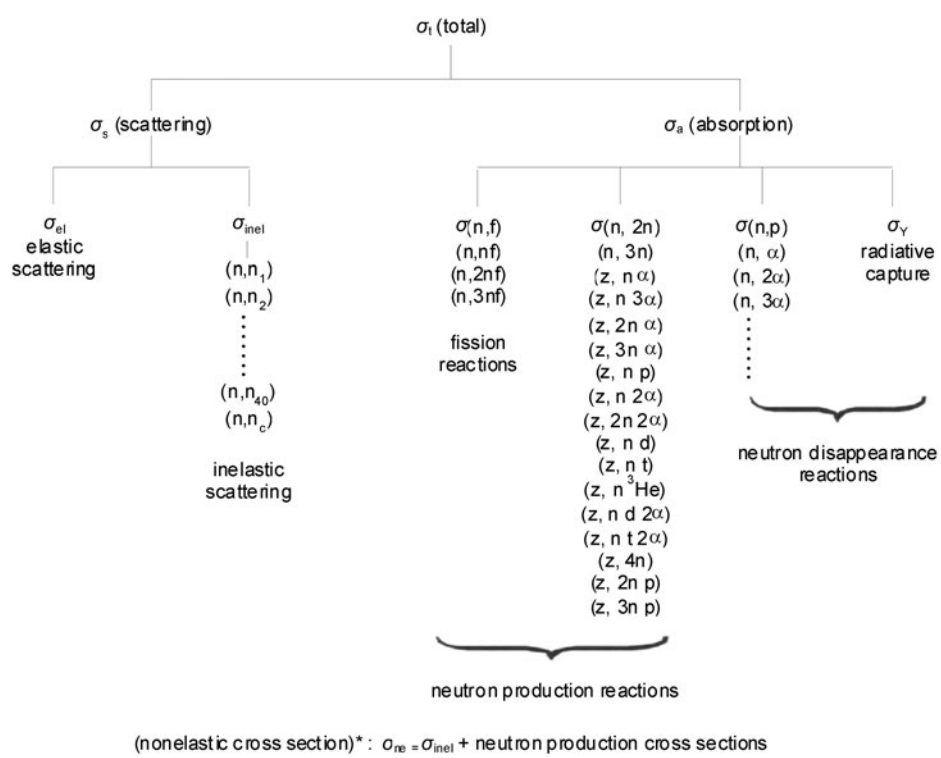

Fig. 1. Cross-section hierarchy for particle interactions.

where

$\bar{\nu}^i(E)$ = average number of neutrons released per fission for the i'th (selected) nuclide at energy E

$\sigma_f^i(E)$ = microscopic fission cross section for the i'th (selected) nuclide at energy E

$P_{fiss}(E)$ = fission probability of the neutron at energy E.

In the multigroup mode, the energy variables in Eqs. (36), (37), and (38) are replaced by energy group index g. The nonabsorption, absorption, and fission probabilities are sometimes referred to as the collision probabilities.

If the neutron energy is in the URR of the selected target nuclide and probability-table data are available, the collision probabilities are adjusted by sampling the partial reactions from the appropriate probability table and recomputing the total cross section. In particular, the revised or sampled values for scattering, absorption, and fission must be used to calculate the collision weights as defined by Eqs. (36), (37), and (38). Depending on the neutron's weight, splitting and/or roulette are performed as necessary.

To prevent expending excessive computer time tracking low-weight neutrons, Russian roulette is played if the weight of the neutron drops below a preset low weight *WTLOW*. The default value is one-third times the average weight. Neutrons survive Russian roulette with the probability $(W/WTAVG)$, where W is the current weight of the particle, and are assigned an average weight *WTAVG*.

If the weight of the neutron exceeds a preset value *WTHIGH*, the neutron is split into two neutrons, each having a weight equal to one-half the weight of the original neutron. After splitting, only one of the split neutrons is followed. The other neutrons are stored to be tracked at the end of the current generation (i.e., split neutrons are all considered part of the current generation and therefore are tracked as additional particles). This procedure is repeated until the weight of the split neutron is less than the value *WTHIGH*. The default value for the preset high weight is three times the average weight. Both Russian roulette and splitting are techniques for reducing computer time without adding any biasing.

The value of *WTAVG*, and therefore *WTLOW* and *WTHIGH*, can be assigned as a function of position and energy. The position dependence is determined by the BIAS IDs (see Sec. III.G). The values used by KENO are as follows:

DWTAV = 0.5 is the default value of *WTAVG*.

WTAVG = *DWTAV* is the weight given a neutron that survives Russian roulette.

WTLOW = *WTAVG*/3.0 is the value of weight at which Russian roulette is played.

WTHIGH = *WTAVG**3.0 is the value of weight at which neutron is split.

Once the current weights are calculated (w, w_a, w_f), the collision can be processed to determine the type of interaction and the corresponding exiting energy and angle if secondary neutrons are generated. In the multigroup mode, the exit group and angle of the secondary neutron are determined.

The kinematics data in the continuous-energy KENO library are provided in the laboratory or target-at-rest system as opposed to the center-of-mass system. By adhering to the laboratory coordinate system, KENO does not have to transform between different coordinate systems during the random walk; however, the energy and angle representations for elastic and discrete-level inelastic scattering become more complex in the laboratory system. For example, an angular distribution that is isotropic in the center-of-mass system is anisotropic in the laboratory system. Moreover, the secondary energy distribution as a function of exit angle in the laboratory system can be double-valued (i.e., two possible exit energies with respect to a single angle) for energies above the threshold for the reaction. Figure 2 shows the exit energy versus exit cosine in the laboratory system for several incident energies in the double-valued region for ^{7}Li. The range of the double-valued region for all nuclides with inelastic cross sections in the ENDF/B-VII Release 0 library are plotted as a function of atomic weight ratio in Fig. 3. Likewise, a similar double-valued distribution is observed for elastic scattering with hydrogen in the laboratory system if the actual mass ratio is used (i.e., A = 0.99928, as opposed to A = 1.0). Consequently,

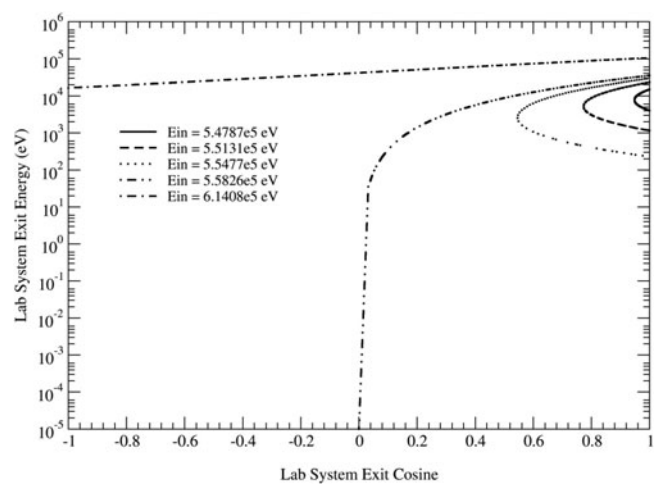

Fig. 2. Exit energy versus exit cosine for selected energies in the double-valued region in the laboratory system for ^{7}Li.

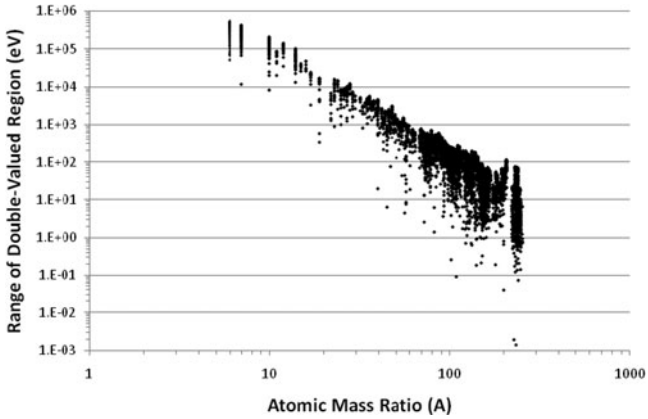

Fig. 3. Range of discrete-level inelastic scattering double-valued region.

when generating the continuous-energy cross sections for KENO, special care is exercised in the construction of the secondary angle and energy distributions in the laboratory system.

After selecting the nuclide for interaction according to Eq. (35) and calculating the weights using Eqs. (36), (37), and (38) to determine if the particle is to be killed or scattered, the collision is modeled using the following procedures.[1]

Reaction Selection

At each collision site, the type of collision must be selected based on the cross-section data. Moreover, the k'th reaction can be randomly selected using the relation in Eq. (39):

$$\sum_{j=1}^{k-1} \sigma_j(E) < R \sum_{j=1}^{NI} \sigma_j(E) \leq \sum_{j=1}^{k} \sigma_j(E) \quad , \tag{39}$$

where

$\sigma_j(E)$ = cross section for the j'th reaction at energy E

NI = number of elastic and nonelastic reactions (i.e., excludes neutron disappearance reactions).

Note that the fission reactions (e.g., total fission, first-chance fission, second-chance fission, etc.) are excluded from Eq. (39) because an implicit approach is used to treat fission. The details of the fission treatment are provided in Sec. III.E. If a neutron production reaction with multiple exit neutrons [e.g., $(n,2n)$, $(n,3n)$, etc.] is selected, the weight of the neutron is adjusted by the multiplicity to account for the additional neutrons [e.g., $w = 2w$ for $(n,2n)$, $w = 3w$ for $(n,3n)$, etc.].

Exit Angle Selection

The cross-section library provides a kinematics data block with a flag that indicates the number of secondary angles for each incident neutron energy. If the value of this flag is 1 and the corresponding cosine value is -2, then the reaction is flagged to be isotropic since the cosine value of -2 is mathematically not possible. The cross-section library also provides the energy distributions of secondary particles for each angle for a specified reaction. The exiting angle for the collision can be obtained as follows:

1. Isotropic emission—The exiting angle cosine is sampled uniformly between -1 and $+1$:

$$\mu = 2R - 1 \quad . \tag{40}$$

2. Anisotropic emission—The exiting angle cosine must be sampled from an anisotropic distribution that is provided in the cross-section library for the specified reaction.

The secondary angular distribution data are provided as a function of incident energy. The initial record of each section for a reaction provides the number of incident energies *NE* for the secondary angular and energy distributions. Corresponding to each incident energy is a secondary angular distribution.

For each angular distribution record, there is an *LMU* flag and an *NPU* flag that describe the format of the data. The *LMU* flag designates whether the secondary distribution is provided in equiprobable cosine bins or in nonequiprobable cosine bins. The *NPU* flag specifies the number of cosine values in the distribution. Based on the incident energy of the neutron, the angular distribution data are sampled from two distributions that bracket the incident energy. The exiting angle cosine μ in the laboratory system is then determined by linearly interpolating between the sampled values.

Exit Energy Selection

In addition to the angular distributions of the kinematics data, the cross-section library provides the energy distributions of secondary particles for a specified reaction. The secondary energy distributions are provided as a function of incident energy and secondary angle cosine in each section. Once the exiting angle cosine is selected, the exiting energy is selected from the energy distribution that corresponds to the (E, μ) pair.

For each energy distribution record, there is an *LE* flag and an *NPE* flag that describe the format of the data. The *LE* flag designates whether the secondary distribution is provided in equiprobable energy bins or in nonequiprobable energy bins. The *NPE* flag specifies the number of secondary energy values in the distribution. For elastic scattering and discrete-level inelastic scattering, the *NPE* flag is equal to the *NPU* flag due to the one-to-one correspondence between angle and energy.

Azimuthal Angle Selection

Azimuthal angle η is selected uniformly between 0 and 2π (i.e., $\eta = 2R\pi$, where R is a random number).

Direction Cosine Calculation

Calculate the new direction cosines in the laboratory system using Eqs. (41), (42), and (43):

$$u' = u\mu - \sqrt{v^2 + w^2}\sqrt{1 - \mu^2}\cos(\eta) \ , \tag{41}$$

$$v' = v\mu + \frac{uv}{\sqrt{v^2 + w^2}}\sqrt{1 - \mu^2}\cos(\eta) - \frac{w}{\sqrt{v^2 + w^2}}\sqrt{1 - \mu^2}\sin(\eta) \ , \tag{42}$$

and

$$w' = w\mu + \frac{uw}{\sqrt{v^2 + w^2}}\sqrt{1 - \mu^2}\cos(\eta) + \frac{v}{\sqrt{v^2 + w^2}}\sqrt{1 - \mu^2}\sin(\eta) \ , \tag{43}$$

where

u, v, w = initial direction cosines

u', v', w' = exiting direction cosines

μ = cosine of the scattering angle

η = azimuthal angle.

When a neutron is scattered in the multigroup mode, a new energy group is selected from the cumulative transfer probability distribution. This group-to-group transfer determines an angular scattering distribution, usually expressed as a Legendre expansion of the cross-section transfer array. A set of discrete angles and probabilities is generated by a generalized Gaussian quadrature procedure, preserving the moments of the Legendre expansion of the angular scattering distribution. Minor adjustments can be made to the moments of the Legendre expansion to avoid negative values. KENO treats P_0 and P_1 Legendre expansions as special cases. If the scattering distribution is isotropic, a flag is set to randomly select new direction cosines from an isotropic distribution, instead of using discrete scattering angles. If the distribution is a P_1 expansion, KENO randomly selects the cosine of the scattering angle according to

1. $|\bar{\mu}| < 10^{-10}/3$: average direction cosine is nearly zero, which is somewhat arbitrarily defined to be $1/3 \times 10^{-10}$, and therefore scattering distribution is isotropic

2. $|\bar{\mu}| \leq 1/3$: $\mu = \left(\sqrt{1 + 6\zeta\bar{\mu} + (3\bar{\mu})^2} - 1\right)/3\bar{\mu}$

or

3. $|\bar{\mu}| > 1/3$: $\mu = \zeta(1 - \bar{\mu}) + \bar{\mu}$,

where

ζ = uniform random variable between -1 and $+1$

$\bar{\mu}$ = mean cosine of the scattering angle.

Otherwise, selection is performed according to the same procedures as in the continuous-energy mode that are described above.

III.E. Fission Treatment

As noted in Sec. III.D, an implicit approach is used to treat a fission event. During the collision treatment, the fission weight is calculated using Eq. (38). After processing the collision, the fission weight is evaluated to determine if the fission treatment should be applied. If the fission weight is greater than zero, the collision occurred in material containing at least one fissile isotope. During the random walk, several fission source points must be generated to provide an adequate representation of the true source distribution. A minimum production factor *mpf* is defined at the beginning of each generation to ensure that enough fission points are generated:

$$mpf = \left(1 - \frac{3.0}{\sqrt{NPG}}\right)\bar{k} \ , \tag{44}$$

where

$\bar{k}$ = running average of k_{eff} through the current generation (1.0 for first two generations)

NPG = number of histories (particles) per generation.

Equation (44) represents a rough estimate of the 99% lower confidence interval for the distribution of the generation k_{eff}. This factor is a function of the square root of the number of neutrons per generation and was chosen because it usually produces an adequate number of independent fission points and does not produce so many that an excessive amount of time is spent choosing from the fission points that are produced.

If the fission weight is greater than zero, a pseudo-fission weight *pfw* is calculated as follows:

$$pfw = \frac{w_f}{R} = \frac{\overline{\nu^i}(E)\sigma_f^i(E)}{R\sigma_t^i(E)} w_b \ . \tag{45}$$

If the pseudo-fission weight is less than the minimum production factor that is given by Eq. (44), fission points are not generated, and tracking of the particle continues. However, if the fission weight is greater than the minimum production factor, *pfw* is redefined to be the minimum production factor divided by a random number:

$$pfw = \frac{mpf}{R} \quad . \tag{46}$$

Once the pseudo-fission weight is redefined, a fission point can be generated. If the mixture is defined by multiple nuclides, the target nuclide is selected based on the fission cross sections as follows:

$$\sum_{j=1}^{i-1} \Sigma_f^j(E) < R \sum_{j=1}^{N} \Sigma_f^j(E) \leq \sum_{j=1}^{i} \Sigma_f^j(E) \quad , \tag{47}$$

where N is the number of different nuclides in the mixture.

After the target nuclide is selected, the exit angle and energy from the fission reaction with that nuclide is sampled. If the selected nuclide has both prompt and delayed neutron spectrums available, the type of spectrum is randomly sampled. Note that the user may force the use of a prompt neutron spectrum. If the chosen spectrum type is prompt neutron spectrum and the nuclide has first-chance, second-chance, etc., fission data available, one of the chance-fission distributions is randomly selected. Then, the fission reaction at the current neutron energy is sampled to determine the exit energy and angle. Each time a fission point is generated, the pseudo-fission weight is stored with the point in the fission bank. The quantity of fission points kept to be used as fission positions for the next generation is limited to the number of positions in the fission bank (input parameter *NFB*). Typically, *NFB* is equal to the input parameter *NPG*, the number of neutrons per generation. Before storing the point, the fission bank must be checked for an available storage location. If the fission bank is full, the bank is searched for the smallest pseudo-fission weight that is subsequently compared with the pseudo-fission weight of the new fission point. The point with the largest *pfw* value is stored in the fission bank. If the pseudo-fission weight of the new point is less than all *pfw* values in the bank, the new point is not stored. If the fission bank is not full or an available storage location is found, the fission point is stored in the bank. When a new point is stored in the fission bank, the energy and angular cosine must be selected from the kinematics data, as described above. In the multigroup mode, the energy group of fission is chosen randomly from the fission spectrum of the mixture in which the fission occurred. Once the neutron data are stored for the new fission point, the fission weight of the history is decremented by the minimum production factor. If the remaining fission weight is greater than zero, the fission treatment procedures are repeated until the fission weight of the history has been exhausted.

When the next generation is ready to be processed, data are transferred from the fission bank into the neutron bank to be used as starting positions for the fission neutrons. If more than *NPG* neutrons are saved in the fission bank, *NPG* of those having the highest values of *pfw* will be used. If too few fission positions were stored (less than the number per generation), a warning message to that effect is printed, and additional fission points are randomly chosen from those that were stored until the number of fission points available to start the next generation is equal to the number of neutrons per generation.

III.F. System Eigenvalue and Other Estimators

The generation k_{eff} for generation n is calculated by

$$k_n = \frac{\sum_{NPG} w_f}{NPG} \quad , \tag{48}$$

where fission weights are summed over number of particles sampled at that generation. The running average k_{eff} of active generations is calculated by

$$\bar{k} = \frac{\sum_{AG} k_n}{AG} \quad , \tag{49}$$

where

AG = number of active generations

$\bar{k}$ = average k_{eff} over AG active generations.

Both average k_{eff} and generation k_{eff} values are listed in the output. In addition, at the completion of all generations, k_{eff} values as a function of generations run and generations skipped are shown in text-based plots in the output. Analysis of the generation k_{eff} values is performed to determine the best system value with the smallest standard deviation by determining the number of generations that should be skipped. Note that the HTML output, if requested, contains a graphical representation of the evolution of the k_{eff} values as well as other indicators that can be viewed as images and copied into other documents.

In addition, system parameters such as average fission group, energy of average lethargy of fission, system mean free path, and system average number of neutrons per fission event as well as neutron lifetime and generation time are calculated and listed. Note that the neutron lifetime and generation time are not the usual kinetics parameters. Rather, the lifetime is the average life span of a neutron (in seconds) from the time it is born until it is absorbed or leaks from the system. The generation time is the average time (in seconds) between successive neutron generations.

III.G. Biasing or Weighting

A study by Hoffman[2] shows the default weight values used in KENO to be reasonable for bare critical assemblies. Figure 4, taken from this study, shows the analytic relationship between the variance and *WTLOW* when *WTAVG* is 0.5. Note that the default value of 0.167 for *WTLOW* is very close to the minimum point on the

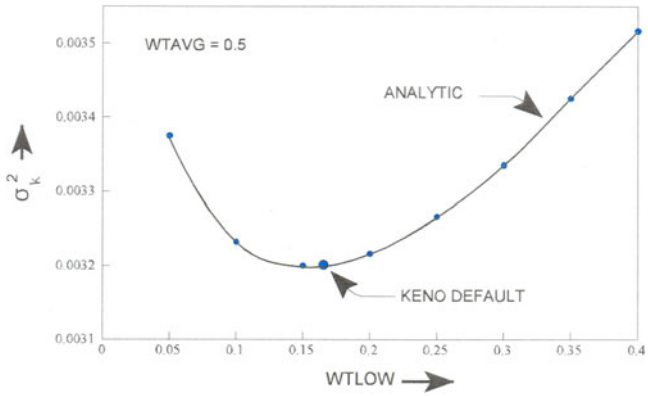

Fig. 4. Analytic estimate of the relationship between *WTLOW* and the variance σ_k^2 when *WTAVG* is 0.5.

curve. Experimental results of actual Monte Carlo calculations[3] for a wide variety of critical systems provide further assurance that 0.167 is an excellent general choice for *WTLOW* when *WTAVG* is 0.5.

Figure 5, also from the Hoffman study, shows the analytic relationship between the variance and the value chosen for *WTAVG* for a value of *WTLOW* = 1/6. Although the KENO default value for *WTAVG* is not the optimum, a close examination of the data shows the variance to be changing relatively slowly as a function of the value of *WTAVG*. Even though this study shows a value near 0.26 to be optimum for the system examined, it is not optimum for all types of systems. Further studies of a wide variety of system types would be needed before changing the default value of *WTAVG* from the 0.5.

Inside a fissile core, the importance of a neutron is a slowly varying function in terms of energy and position. Hence, for many systems, the standard defaults for *WTLOW* and *WTAVG* are good values to use. For reflectors, however, the worth of a neutron varies both as a function of distance from the fissile material and as a function of energy. As a neutron in the reflector becomes less important relative to a neutron in the fissile region, it becomes desirable to spend less time tracking it. Therefore, a space- and energy-dependent weighting or biasing function is used in KENO to allow the user to minimize the variance in k_{eff} per unit tracking time. When a biasing function is used in a reflector, it becomes possible for a neutron to move from one importance region into another whose *WTLOW* is greater than the weight of the neutron. When this occurs, Russian roulette is played to reduce the number of neutrons tracked. When the reverse occurs, that is, the neutron moves to a region of higher importance, its weight may be much higher than *WTAVG* for that region. When the weight of the neutron is greater than a preset value *WTHIGH*, the neutron is split into two neutrons, each having a weight equal to one-half the weight of the original neutron. This procedure is repeated until the weight of the split neutron is less than *WTHIGH*. *WTHIGH* is the weight at which splitting occurs.

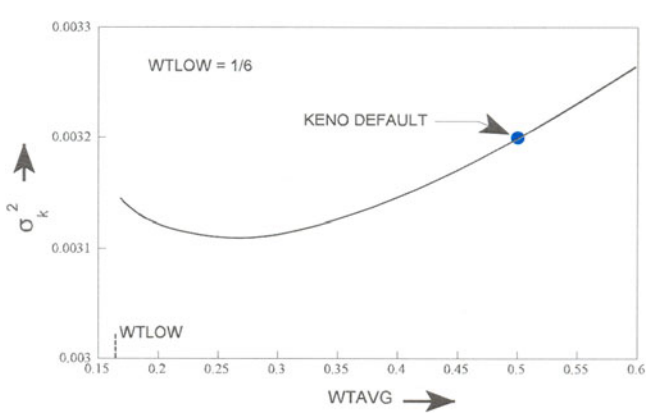

Fig. 5. Cross-analytic estimate of the relationship between *WTAVG* and the variance σ_k^2 when *WTLOW* is 1/6.

The weighting or biasing function for a given core material and reflector material can be obtained by using the adjoint solution from discrete ordinates codes for a similar (usually simplified) problem. This adjoint flux gives the relative contribution of a neutron at a given energy and position to the total fissions in the system. The weighting function for KENO is thus proportional to the reciprocal of the adjoint flux. Although such a function can be difficult to obtain, the savings gained makes the effort worthwhile for many of the materials that are frequently used as reflectors. Biasing functions have been prepared for several reflector materials commonly used in KENO calculations. The use of biasing to minimize the variance in k_{eff} per unit computer time will usually increase the variance in other parameters such as leakage or absorption in the reflector.

III.H. Differential Albedos

Arrays reflected by thick layers of material having a small absorption-to-scattering ratio may require large amounts of computer time to determine k_{eff} because of the relatively long time a history may spend in the reflector. A differential albedo technique, which is currently available for multigroup mode calculations only, was developed for use with the KENO codes to eliminate the need for tracking particles in the reflector. This involves returning a history at the point it impinges on the reflector and selecting an emergent energy and polar angle from a joint density function dependent upon the incident energy and polar angle. The weight of the history is adjusted by the functional return from the reflector, which is also based on the incident energy and angle.

The characteristics of a differential albedo emulate the attributes of the reflector material and are independent of the material or materials adjacent to the reflector. Thus, a differential albedo that is generated for a given

reflector material can be used with any array, regardless of the type of fuel or fissile material contained within the array.

For many calculations involving reflected arrays of fissile material, the differential albedo treatment is a powerful tool that can significantly reduce the computing time required to determine k_{eff}. The savings will naturally vary, depending on the importance of the reflector to the system. A substantial effort is required to generate a differential albedo, but the savings gained are well worth the effort for commonly used reflector materials.

To generate the differential albedo information for a material, a fixed-source calculation must be made for each incident energy and angle. The data presently available for use with KENO were generated by 1-D discrete ordinates calculations for slab geometry, representing infinite slabs. Consequently, for a finite reflector, these data will not correctly treat histories that enter the reflector near an edge or corner. Past experience with differential albedo reflectors indicates that k_{eff} appears to be conservative for small faces and will tend toward the correct result as the face becomes large relative to the area near the corners. Care must be taken to ensure that any surface to which a differential albedo is applied is large enough that the errors at the edges can be ignored.

Because differential albedos are time-consuming to generate, those corresponding to the Hansen-Roach 16-energy-group structure are the only differential albedos currently available for use with KENO. In the past, their use was limited to problems utilizing cross sections having the Hansen-Roach 16-energy-group structure. KENO extends the use of differential albedos to other energy-group structures by allowing appropriate energy transfers. This is accomplished by creating lethargy boundary tables for the albedo group structure and the cross-section group structure and determining the lethargy interval corresponding to the desired transfer (cross-section group structure to albedo group structure or vice versa) based on a uniform lethargy distribution over the interval. When the energy-group boundaries of the cross sections and albedos are different, the results should be scrutinized by the user to evaluate the effects of the approximations.

III.I. Fluxes

Fluxes are computed in KENO with a track-length estimator from all active generations (all but user-defined number of generations that are skipped). The scalar flux in region z for energy group g for a single generation is computed as

$$\Phi_{g,z} = \frac{\sum_{k=1}^{K} W_{k,z} l_{k,z}}{V_z \sum_{k=1}^{K} W_{k,0}} , \tag{50}$$

where

$l_{k,z}$ = distance traversed by particle k while within region z and energy group g

$W_{k,z}$ = weight of particle k while traversing region z

V_z = volume of region z

$W_{k,0}$ = initial weight of particle k

K = total number of histories in the generation.

The average fluxes for all active generations and the standard deviation in the averages are also computed.

KENO is also capable of computing the angular flux for a symmetric-level quadrature set. The angular flux for energy group g in region z for quadrature direction n is computed as

$$\Phi^n_{g,z} = \frac{\sum_{k=1}^{K} W_{k,z} l_{k,z,n}}{V_z \sum_{k=1}^{K} W_{k,0}} , \tag{51}$$

where $l_{k,z,n}$ is the distance traversed by particle k while within region z and energy group g within the quadrature direction bin n.

The angular flux can be expanded to a flux moment using an appropriate spherical harmonics expansion. KENO has even number symmetric-level quadrature sets S_2 through S_{16}.

Flux moments can also be computed directly in KENO. The j'th moment, corresponding to real-valued spherical harmonics functions for a single generation for energy group g in region z, is computed as

$$\tilde{\phi}^j_{g,z} = \frac{\sum_{k=1}^{K} R^j_k W_{k,z} l_{k,z}}{V_z \sum_{k=1}^{K} W_{k,0}} , \tag{52}$$

where R^j_k is the real-valued spherical harmonics function for moment index j corresponding to the direction of particle k.

KENO offers the option of computing the angular fluxes and flux moments using a transformed coordinate system such that the moments are based on a polar rather than a Cartesian position vector. This is a three-dimensional (3-D) extension of the 1-D method for calculating the flux moments in terms of Legendre polynomials based only on the direction cosine with respect to the spatial coordinate.

This coordinate transform is illustrated in Fig. 6, where $\hat{i}$, $\hat{j}$, and $\hat{k}$ represent the directional coordinate system axes; μ, η, and ξ represent the direction cosines; and θ and ρ represent the polar and azimuthal angles of the "normal" coordinate system. The same symbols "primed" represent the transformed coordinate system. Here, the

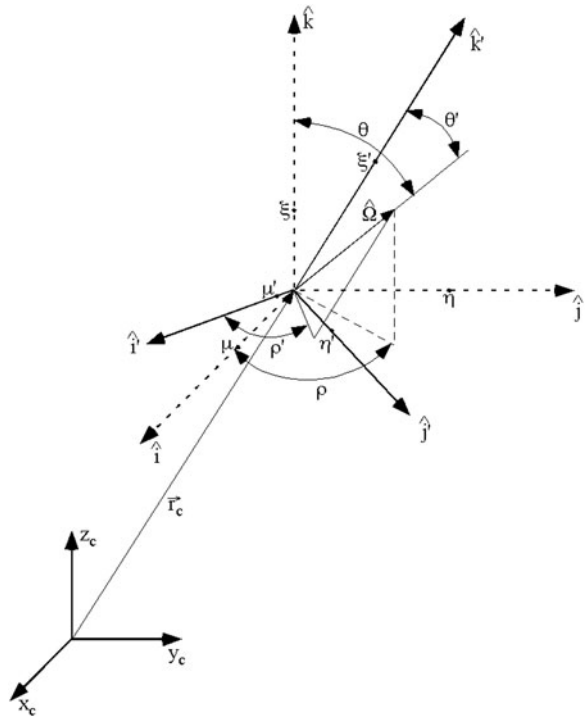

Fig. 6. Coordinate transform used for quadrature direction and spherical harmonics terms.

transformed polar or $\hat{k}'$ axis is colinear with the position vector $\vec{r}$ directed from the center of the region for which moments are desired to the point at which the flux tally occurs. By using the center of the region as a reference point, consistency of the moment calculation is ensured with differing models of the same system. The $\hat{i}'$ and $\hat{j}'$ axes are chosen to form an orthogonal coordinate system with $\hat{i}'$ held in the plane formed by $\hat{i}$ and $\hat{j}$. The use of constraints other than the restriction of $\hat{i}'$ to this plane may be explored in future studies. If an additional constraint is not placed on either $\hat{i}'$ or $\hat{j}'$, the transform would be able to rotate about $\hat{k}'$, and the consistency of consecutive transformations of the same direction could not be ensured. With the transform computed, the position and direction of travel of the particle remain unchanged, but the quadrature directions and/or spherical harmonics terms are calculated using the transformed coordinate system. With the direction cosines consistently transformed for each history, the new polar and azimuthal angles can be computed, and the spherical harmonics functions can be calculated for each history.

KENO offers a mesh flux tally where the fluxes are computed in a user-defined cubic mesh superimposed on the geometry model. The mesh is defined from the origin of the global unit and is oriented with the Cartesian axes. At the end of each particle track, appropriate track lengths are assigned to the mesh intervals that were crossed for the region in which the track occurred. The length of the actual particle track is equal to the sum of the lengths assigned to the meshes encountered by the particle track. Because the coordinates of the mesh are defined in terms of the global unit, fluxes for regions in repeated units (i.e., units in arrays or holes) may be stored separately for each occurrence of the unit. The volumes of each region in each mesh interval are computed such that the fluxes are appropriately normalized on a per-unit-volume basis, consistent with Eq. (51). When the mesh flux option is activated, all requested fluxes, scalar, angular, and/or moment, are computed for each mesh interval.

III.J. Statistical Uncertainty

The statistical uncertainty calculated by KENO is the standard deviation of the mean. This assumes a large sample having a normal distribution. KENO calculates the real variance using an iterative approach and lag covariance data between generations as follows[4,5]:

Step 1: The sample variance and covariance estimates are calculated.

Step 2: The apparent variance is set equal to the sample variance, and the apparent covariance is set equal to the sample covariance.

Step 3: The real covariance is set equal to the apparent covariance, and the real variance is calculated.

Step 4: Using the real variance and apparent covariance, the real covariance is calculated.

Step 5: The real variance is recalculated.

Step 6: Steps 4 and 5 are repeated until the real variance converges within a preset tolerance. The covariance estimates are calculated only for the previous 20 generations. A maximum of 50 iterations is allowed for the real variance to converge.

III.K. Probability Table Treatment

For each isotope with unresolved resonance data, multiple probability tables may be used to describe the URR in the continuous-energy-mode calculations. The header block in the cross-section file for each isotope has a flag that provides the number of probability tables for an isotope. Each table is defined for an incident energy E_i. For a particle with energy E, a search must be performed to find the probability tables with incident energies that bracket the particle energy (i.e., $E_i \leq E < E_{i+1}$). Once the appropriate tables are identified, the tables are sampled to obtain the total, elastic scattering, fission, and capture cross-section values in the URR (Ref. 6).

The probability-table block in the cross-section file provides four separate records that correspond to each reaction within a table: total, elastic, fission, and capture. However, the probability-table construction is based on the total cross section. Therefore, the probabilities in

each table refer to the total cross-section band values, and the bands are sampled based on the total cross section. Once the band for the table corresponding to the energy E_i is sampled, the corresponding partial reaction cross-section values are selected from the same band as the total cross section. The cross-section values for the same band are selected from the table corresponding to the energy E_{i+1} as well. The final total and partial cross-section values are determined by linear interpolation between E_i and E_{i+1} table values.

IV. KEY FEATURES

This section describes the features such as geometry options, restart capabilities, system analysis with fission matrix information, adjoint mode calculations, and two-dimensional (2-D) slice plots.

IV.A. Geometry

IV.A.1. KENO V.a

Because of its speed, KENO V.a is widely used even though it is restricted to the use of specific shapes. These shapes are called geometry regions or regions. Allowed shapes are cubes, cuboids (rectangular parallelepipeds), spheres, cylinders, hemispheres, and hemicylinders. These shapes must be oriented along orthogonal axes and cannot be rotated. They can be translated. Hemispheres and hemicylinders are not limited to half-spheres and half-cylinders; the definitive plane can be positioned by entering a chord. The value of this chord can range from the positive magnitude of the radius (giving a complete sphere or cylinder) to the negative magnitude of the radius (giving a zero volume, nonexistent sphere or cylinder).

A major restriction applied to KENO V.a geometry is that intersections are not allowed. Furthermore, each successive geometry region must completely enclose the preceding region. Tangency and shared faces are allowed. The volume of a region is the volume of the specified shape minus the volume of the preceding region shape and any holes contained in the region. To alleviate the complete enclosure restriction, KENO V.a allows multiple sets of geometry regions with each set independently governed by this restriction. Each set of these multiple geometry regions is called a unit. Units can be stacked together in 3-D rectangular arrays or lattices. Units that are to be stacked together in this manner must have a rectangular parallelepiped outer region, and the adjacent faces of adjacent units must be the same size and shape. An array can be treated as a unit and used within another array; this is called nesting.

The use of holes in KENO V.a allows a unit to be emplaced within another unit, thereby alleviating the restriction that each region within a unit must completely enclose all preceding regions within that unit. However, a hole is not allowed to intersect other holes or regions. A unit that is to be used as a hole need not have a rectangular parallelepiped as its outer boundary. A hole is not a void space since a unit actually occupies the space in it.

Multiple arrays can be described in KENO V.a. The global array in an unreflected problem is the outermost array in the problem geometry description. The global array in a reflected problem is the array referenced by the global unit.

Consistent with past versions, KENO V.a retains the capability of running a single-unit problem. A single-unit problem is one that has no array description or holes.

IV.A.2. KENO-VI

KENO-VI geometry can model any geometric shape that can be described using quadratic equations. These geometric shapes are stacked together forming regions. The set of regions is then used to build units. A set of predefined shapes that include cones, cuboids, cylinders, dodecahedrons, ecylinders (elliptical cylinders), ellipsoids, hexprisms, hoppers, parallelepipeds, planes, rhombohedrons, rhexprisms (rotated hexprisms), spheres, and wedges, as well as others, is used to construct regions. In addition, the keyword quadratic is provided to input surfaces composed of the generalized quadratic equation. These surfaces can be used to construct additional shapes not presently contained in KENO-VI. All shapes and surfaces can be rotated and translated to any orientation and position within their respective unit. Hemispheres and hemicylinders can be constructed using spheres and cylinders with one or more chords. Surfaces and equations are rotated using angles associated with the Euler X-convention and translated by providing a new position for the origin.

A major improvement in KENO-VI is the ability to intersect regions. This is done by specifying whether a particular region is inside or outside each body or surface in the unit. Only those bodies and surfaces that are necessary to define the region must be specified. Additionally, a unit boundary volume must be specified for each unit. Only the volume contained in the boundary volume is considered part of the unit. Like KENO V.a, each unit is independent; however, in KENO-VI, a global boundary must be specified for each problem, including a single unit problem. Unlike KENO V.a, region volumes are no longer analytically calculated because of the complexity involved with intersecting regions. Each region volume can be specified in the input or statistically calculated using random points or rays.

Arrays in KENO-VI are significantly more flexible and complex than in KENO V.a. Arrays may be composed of either cuboids, hexprisms, rhexprisms, or dodecahedrons. Like KENO V.a, the faces of adjacent units in an array must have the same size. This means that all hexprisms, rhexprisms, or dodecahedrons that make up an array must be of the same size. An array boundary must

be specified for each array, and only that portion of the array within the boundary is considered a part of the system. Also, the specified array must fill all the volume in the specified array boundary. The array boundary may be any shape that can be specified using quadratic equations.

The use of holes is also more flexible in KENO-VI. Like KENO V.a, within a unit, holes cannot intersect other holes or the unit boundary, but they can intersect region boundaries. The use of holes is not necessary to build complex geometries; they are used primarily to more efficiently build complex geometries and reduce the amount of computer time needed for the problem. In KENO-VI the crossing to each surface in the unit must be calculated after each collision. The number of surfaces in a unit and the number of collisions in the unit are directly proportional to the amount of CPU time required for the problem. By moving some of the surfaces in a unit into another unit that is included as a hole, all the surfaces in the hole unit except the outer boundary are removed from the containing unit. The judicious use of holes in KENO-VI can significantly speed up the calculation.

Multiple arrays can be described in KENO-VI. If a global array is desired or needed for start or matrix data, it must be specified. In KENO-VI the outermost boundary is always specified as the global-unit boundary. If the outermost boundary is to be the array boundary, a global unit must still be specified, with the global-unit boundary coinciding with the array boundary. Unlike past versions of KENO, KENO-VI cannot run a single-unit problem without specifying a global unit.

IV.B. Restart

KENO incorporates a versatile and convenient restart capability. The decision to write a restart file requires the user to specify only the number of generations between writing restart data and the unit number where the restart file is to be written. The input data, which describe the problem, are the first data written on the restart data file. After the input data have been written on the restart data file, the calculated data are written to a second file at the end of each specified generation. These data include the generation number, random number, number of histories per generation, number of energy groups, bank lengths, common information, the k_{eff}'s by generation, the neutron bank, the fission densities, matrix arrays, and the calculated group-dependent data. These group-dependent data are written a group at a time and include leakages, absorptions, fissions, and fluxes.

The KENO restart capability allows a problem to be restarted at the first generation with different input because all data input supersedes data from the restart data file.

If a problem is to be restarted at a generation greater than 1, the only data that can be changed are certain parameter data. Changes in the parameter data that are not allowed include (a) requesting fissions and absorptions by region if they were not requested by the parent case, (b) requesting fission densities and fluxes if they were not requested by the parent case, (c) requesting matrix information that was not requested in the parent case, and (d) changing the configuration of the neutron bank to be different from that of the parent case.

If a problem is to be restarted following a generation for which restart data were not written, the code will write a message and restart with the next available generation for which restart data exist. If no such generation is found, the problem is terminated.

IV.C. System Eigenvalue Calculation With Matrix

Matrix k_{eff} calculations provide an additional method of calculating the k_{eff} of the system. Cofactor k_{eff}'s and source vectors, which describe the contribution to the system k_{eff} from each unit, hole, or array, are additional information that can be provided when the matrix k_{eff} is calculated. The necessary source and fission weight data are collected during the course of tracking the neutrons through the system. This information is converted to a fission production matrix, which is the number of next-generation neutrons produced in unit, hole, or array J by a neutron born in unit, hole, or array I. The principal eigenvalue of the fission probability matrix is the matrix k_{eff}. The fission product matrix for any of the four alternatives present in KENO is calculated using the appropriate transport operator as shown in Eq. (53):

$$[A]\hat{X} = \frac{1}{\lambda}\hat{X} \ ,$$

$$A_{ij} = \int \nu\Sigma_f^j \Phi_{ij} \ ,$$

and

$$\Phi_{ij} = \int T_{ij}\nu\Sigma_f^i \Phi_i \ , \tag{53}$$

where

$[A]$ = eigenvalue transport operator

A_{ij} = fissions in position j caused by neutron born in position i

Σ_f^i = fission macroscopic cross section in position i

Φ_{ij} = flux in position j caused by neutrons born in position i

T_{ij} = transport operator from position j to position i

$\sum_i \nu\Sigma_f^i\Phi_i = 1$ = normalization function.

KENO offers four alternatives when calculating the matrix k_{eff}, as follows:

1. If MKP = YES is specified in the parameter data, the fission production matrix is collected by array position or position index in the global array. The position index is used to reference a given location in a 3-D lattice. For a $2 \times 2 \times 2$ array, there are nine unique position indices as shown in Table II. Position zero contains everything outside the global array. The fission production matrix is the number of next-generation neutrons produced at index J by a neutron born at index I. This matrix is used to calculate the matrix k_{eff}, cofactor k_{eff}'s, and the source vector by the position index. Because the size of the fission probability matrix is the square of the array size (for a $4 \times 4 \times 4$ array there are 4096 entries), it can use vast amounts of computer memory.

2. If MKU = YES is specified in the parameter data, the fission production matrix is collected by unit. It is the number of next-generation neutrons produced in unit J by a neutron born in unit I. This matrix is used to calculate the matrix k_{eff}, cofactor k_{eff}'s, and source vector by unit.

3. If MKH = YES is specified in the parameter data, the fission production matrix is collected by hole number. Matrix information can be collected at either the highest hole nesting level (first level of nesting) or the deepest hole nesting level. HHL = YES specifies that the matrix information will be collected at the first nesting level. By default, the matrix information is collected at the deepest nesting level. The fission production matrix is the number of next-generation neutrons produced in hole J by a neutron born in hole I. This matrix is used to calculate the matrix k_{eff}, cofactor k_{eff}'s, and the source vector by hole.

4. If MKA = YES is specified in the parameter data, the fission production matrix is collected by array number. It can be collected at the highest array level (first level of nesting) or at the deepest array level. HAL = YES specifies that the matrix information will be collected at the first nesting level. By default, the matrix information is collected at the deepest nesting level. The fission production matrix is the number of next-generation neutrons produced in array J by a neutron born in array I. This matrix is used to calculate the matrix k_{eff}, cofactor k_{eff}'s, and the source vector by array.

TABLE II

Position Indices

	Position		
	X	Y	Z
0	0	0	0
1	1	1	1
2	2	1	1
3	1	2	1
4	2	2	1
5	1	1	2
6	2	1	2
7	1	2	2
8	2	2	2

The user can simultaneously utilize all methods of calculating the matrix k_{eff}. The results are labeled in the printout. Matrix k_{eff}'s cannot be calculated for a single-unit problem.

A cofactor k_{eff} is the eigenvalue of the fission production matrix, reduced by the row and column that reference the specified unit or position index. The difference between the k_{eff} for the system and the cofactor k_{eff} for a unit or position index is an indication of the in situ k_{eff} of that unit or the contribution that unit makes to the k_{eff} of the system. The cofactor k_{eff} of a unit devoid of fissile material should approximate the k_{eff} of the system.

IV.D. Adjoint Mode Calculations

In the multigroup mode of calculations, KENO offers adjoint mode calculations. In the adjoint mode, for each mixture j, $\nu_g^j \Sigma_{fg}^j$ is normalized to one and stored in $\chi^j(g)$. Likewise, $\chi^j(g)$ is normalized using the same normalization constant and stored in $\nu_g^j \Sigma_{fg}^j$. As a result, the source points for the next generation are selected based on a distribution that looks like the fission spectrum $\chi^j(g)$ normalized to the integral of $\nu_g^j \Sigma_{fg}^j$, and the energy group distribution of the next-generation source neutrons looks like $\nu_g^j \Sigma_{fg}^j$ normalized to one. Figure 7 shows the forward and adjoint $\chi(g)$ and $\nu_g \Sigma_{fg}$ values for ^{235}U in the 238-energy-group structure. Generally, $\chi^j(g)$ is zero below ~1 keV in the forward mode and zero above ~1 eV in the adjoint mode. Consequently, when the adjoint neutron energy group is above the electron-volt range, no positions are selected. Hence, the adjoint mode calculations run longer to achieve the same statistical uncertainty on k_{eff} and may suffer from not storing enough fission points for the next generation. In the adjoint mode, in addition to the adjoint k_{eff}, which should be the same as the forward k_{eff} within statistical uncertainty, the adjoint fluxes may be calculated. Adjoint mode calculations are currently not available in the continuous-energy mode.

IV.E. Plots

Two-dimensional plots of slices specified through the geometry can be generated and displayed (a) as character plots using alphanumeric characters to represent mixture numbers, unit numbers, or bias identification numbers or (b) as color plots that generate a PNG file

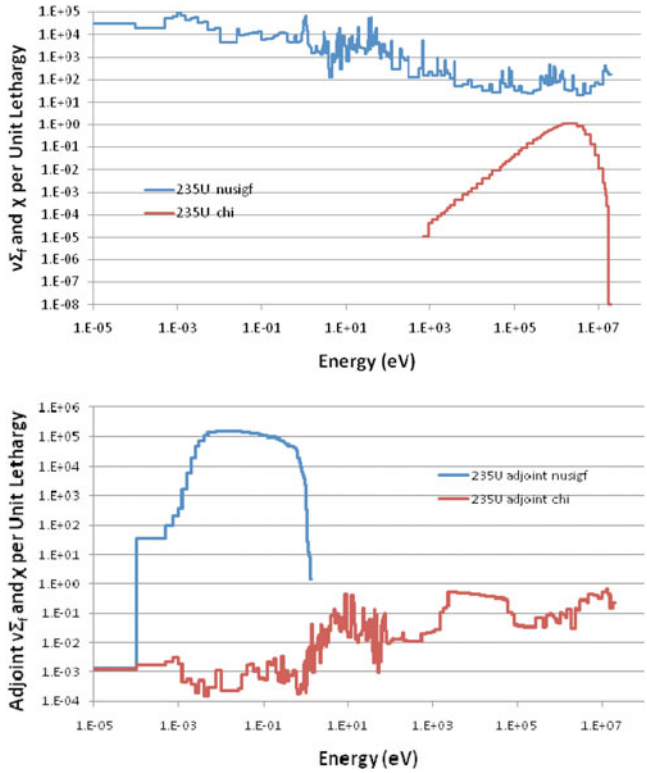

Fig. 7. Forward and adjoint $\chi(g)$ and $\nu_g \Sigma_{fg}$ for ^{235}U in 238-energy-group structure.

using colors to represent mixture numbers, unit numbers, or bias identification numbers.

V. PERFORMANCE AGAINST BENCHMARKS

KENO codes have been tested in both multigroup and continuous-energy modes using hundreds of benchmark cases.[7–10] Benchmark problems referenced below have been selected to provide a validation suite from a wide range of fissile systems. The benchmark problems are divided into six groups: Highly enriched uranium (HEU) systems, intermediate-enriched uranium (IEU) systems, low-enriched uranium (LEU) systems, mixed oxide (MOX) systems, plutonium (Pu) systems, and ^{233}U systems. The benchmark problems are from the "International Handbook of Evaluated Criticality Safety Benchmark Experiments"[11] (IHECSBE). Detailed model descriptions are not provided in this paper but are available in Sec. 3 of the appropriate evaluation in IHECSBE.

A total of 262 benchmark problems have been modeled and analyzed in six groups. All KENO calculations used continuous-energy cross sections based on ENDF/B-VII Release 0 evaluations and have been run with a sufficient total number of histories to achieve a standard deviation of k_{eff} of 0.0005 or less. The performance of the KENO code against these benchmark problems is demonstrated in Figs. 8 through 13, in which the primary Y-axis is the benchmark and KENO-calculated eigenvalues with 2σ error bars. Generally, multigroup mode results are very similar to the continuous-energy-mode results. The exceptions may be due to the inadequacy of the resonance self-shielding treatment due to theory, limitations of the 1-D unit cell models used for cross-section processing, or unidentified differences between the continuous-energy and multigroup cross sections. Identification of the actual reasons would be very time-consuming, as it would require analyzing each case to determine the need, if any, and the applicability of the resonance self-shielding treatment and therefore is deemed beyond the scope of this paper.

Table III lists the average ratios of total execution times between the continuous-energy-mode and multigroup-mode calculations for the six sets of calculations. Generally, the multigroup-mode calculations are about five times faster.

The HEU group consists of 76 benchmarks. Most of the calculated k_{eff} results are within 2σ of the experimental values with three exceptions; these are within 3σ.

The IEU group consists of nine benchmarks. All but one benchmark k_{eff} value is within 2σ of the experimental values. The last case is 4.1σ different, which amounts to ~0.2% difference. The reason for this is unknown and

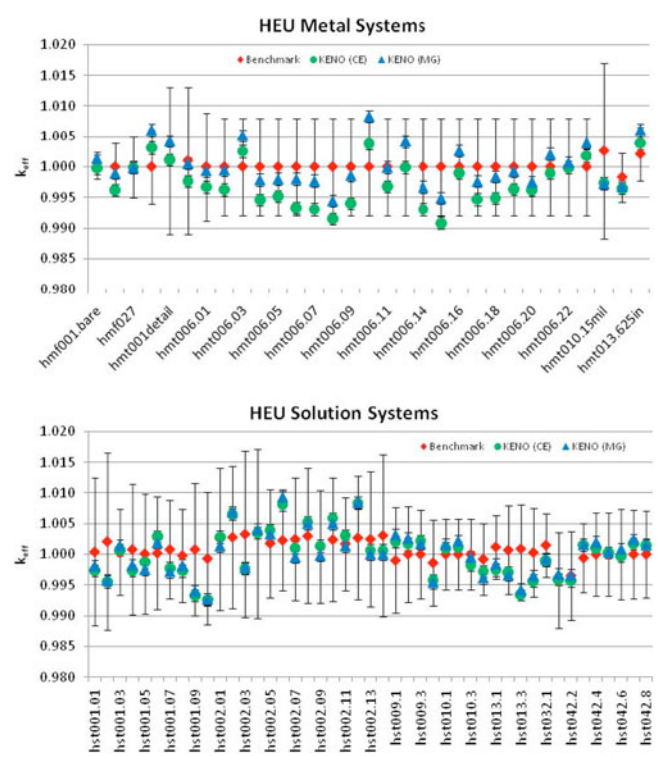

Fig. 8. Calculated eigenvalues and numbers of sigma differences for HEU benchmarks.

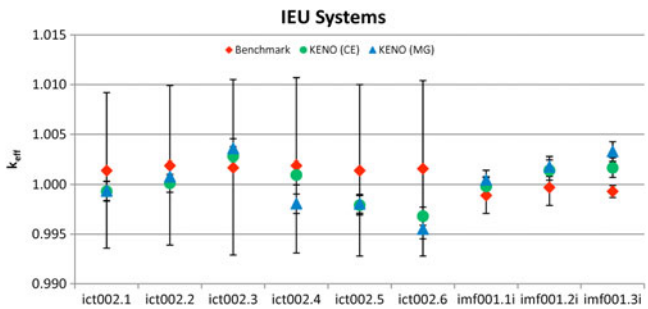

Fig. 9. Calculated eigenvalues and numbers of sigma differences for IEU benchmarks.

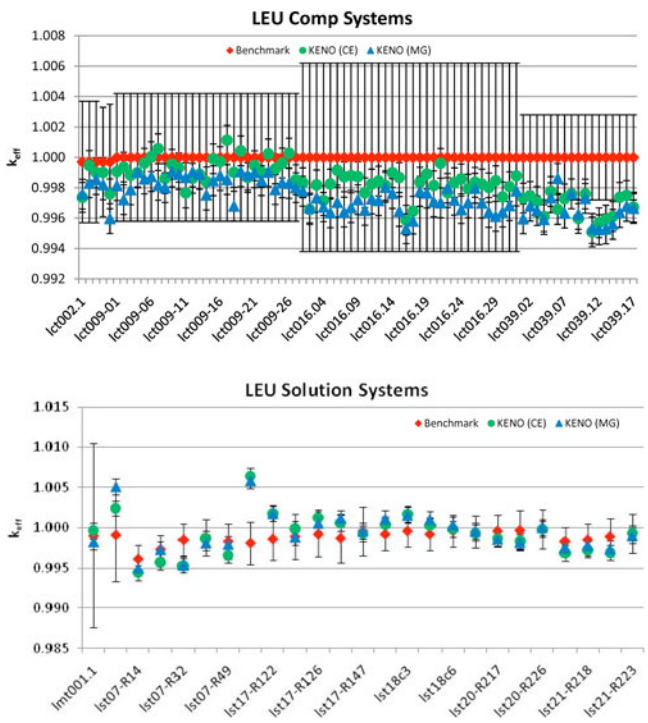

Fig. 10. Calculated eigenvalues and numbers of sigma differences for LEU benchmarks.

may be due to input problems since the other two cases in the same series are calculated more accurately.

The LEU group contains 106 benchmarks. Most of the calculated k_{eff} values are within 2σ of the experimental values. One series of benchmarks designated by LEU-COMP-THERM-039 has k_{eff} differences that are within 3σ of the experimental values. In all LEU benchmark cases that are calculated for this paper, one case stands out with a very large difference. Case 104 of LEU-SOL-THERM-17 shows $\sim 6\sigma$ difference between the benchmark k_{eff} value and the experimental value. Published results of this series of benchmarks exhibit similar differences in their calculations.[11]

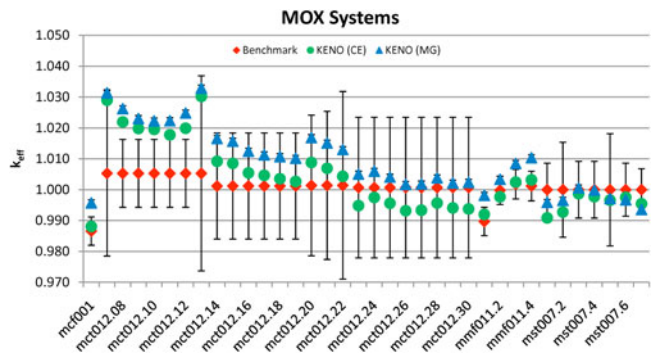

Fig. 11. Calculated eigenvalues and numbers of sigma differences for MOX benchmarks.

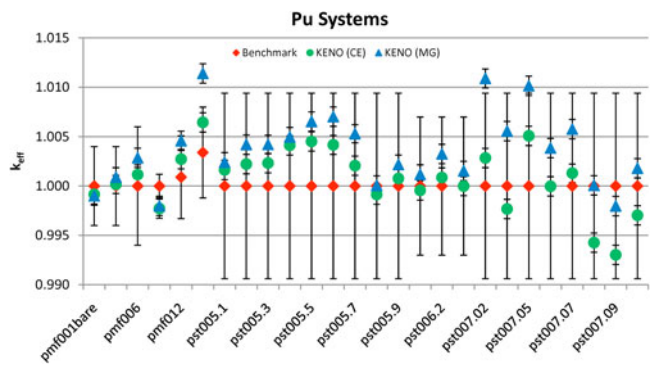

Fig. 12. Calculated eigenvalues and numbers of sigma differences for Pu benchmarks.

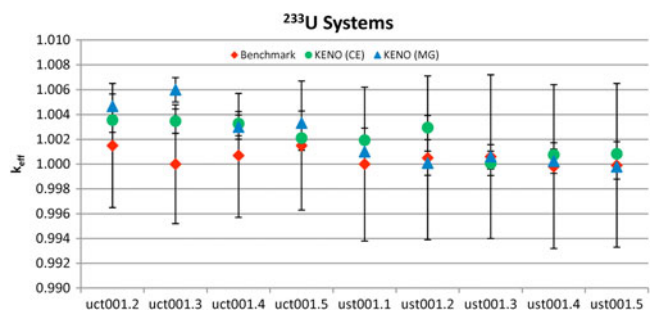

Fig. 13. Calculated eigenvalues and numbers of sigma differences for ^{233}U benchmarks.

The MOX group contains 36 cases, with most of the calculated k_{eff} values within 2σ of the experimental values. The rest of the cases are calculated within 3σ of the benchmark values.

The Pu group consists of 26 benchmarks. All but one are calculated within 2σ. The case Pu-MET-FAST, 008-1 is within 3σ, which is $\sim 0.2\%$ different.

TABLE III

Average Ratio of Total Execution Times

	Continuous Energy/ Multigroup
HEU	6
IEU	2
LEU	5
MOX	6
Pu	6
^{233}U	4

The ^{233}U group consists of nine benchmarks. All of the calculated k_{eff} values are within 2σ of the benchmark values.

VI. SUMMARY

The theory and governing equations for Monte Carlo simulation of a self-multiplying system by KENO codes of the SCALE code system have been outlined. The solution algorithm has been explained by providing details of problem initialization, initial source distribution, and collision site selection during tracking, collision, and fission treatment. Additional features such as biasing, differential albedos, calculation of flux tallies as well as standard deviations, geometry features, restart capabilities, system analysis techniques with matrix, and 2-D plots have been explained.

Performance of both continuous-energy-mode and multigroup-mode calculations has been demonstrated against experimental benchmarks for 262 cases that include HEU, IEU, LEU, MOX, Pu, and ^{233}U systems. No timing studies have been performed as they depend highly on the type of machine and system resources available. All problems were run on various nodes of the CPILE2 Linux cluster at Oak Ridge National Laboratory, which uses the 64-bit Redhat Enterprise Linux version 4.7 operating system. Each node has a minimum of 16 GB of memory. In general, the multigroup mode uses two to six times less CPU time than the continuous-energy-mode calculations.

ACKNOWLEDGMENTS

Oak Ridge National Laboratory is managed and operated by UT-Battelle, LLC, for the U.S. Department of Energy under contract DE-AC05-00OR22725.

REFERENCES

1. M. E. DUNN, N. M. GREENE, D. F. HOLLENBACH, and L. M. PETRIE, "Monte Carlo Methods Development for a Continuous-Energy Version of KENO," *Proc. Topl. Mtg. Monte Carlo Method: Versatility Unbounded in a Dynamic Computing World*, Chattanooga, Tennessee, April 17–21, 2005, American Nuclear Society (2005) (CD-ROM).

2. T. J. HOFFMAN, "The Optimization of Russian Roulette Parameters for KENO V.a," ORNL/TM-7539, Union Carbide Corporation (Nuclear Division), Oak Ridge National Laboratory (1982).

3. R. D. O'DELL and R. E. ALCOUFFE, "Transport Calculations for Nuclear Analyses: Theory and Guidelines for Effective Use of Transport Codes," LA-10983-MS, Los Alamos National Laboratory (1987).

4. T. UEKI, T. MORI, and M. NAKAGAWA, "Error Estimations and Their Biases in Monte Carlo Eigenvalue Calculations," *Nucl. Sci. Eng.*, **125**, 1 (1997).

5. L. DEMARET, A. NOURI, L. CARRARO, and O. JACQUET, "Accurate Determination of Confidence Intervals in Monte Carlo Eigenvalue Calculations," *Proc. 6th Int. Conf. Nuclear Criticality Safety (ICNC 99)*, Versailles, France, September 20–24, 1999, Vol. 1, p. 66 (1999).

6. M. E. DUNN and L. C. LEAL, "Calculating Probability Tables for the Unresolved-Resonance Region Using Monte Carlo Methods," *Nucl. Sci. Eng.*, **148**, 1 (2004).

7. T. SUMNER and S. GOLUOGLU, "Verification of KENO V.A and KENO-VI Using Analytical Benchmarks," *Proc. 8th Int. Conf. Nuclear Criticality Safety (ICNC 2007)*, St. Petersburg, Russia, May 28–June 1, 2007, Vol. I, p. 361 (2007).

8. S. GOLUOGLU, M. E. DUNN, N. M. GREENE, L. M. PETRIE, and D. F. HOLLENBACH, "Generation and Testing of the Continuous-Energy Cross-Section Library for Use with Continuous-Energy Versions of KENO," *Proc. 8th Int. Conf. Nuclear Criticality Safety (ICNC 2007)*, St. Petersburg, Russia, May 28–June 1, 2007, Vol. I, p. 364 (2007).

9. S. GOLUOGLU, "Performance of the New Continuous Energy Capability in KENO V.a," *Trans. Am. Nucl. Soc.*, **99**, 407 (2008).

10. S. GOLUOGLU, M. E. DUNN, L. M. PETRIE, and T. S. SUMNER, "Development and Validation of the New Continuous-Energy Capability in the Criticality Safety Code in KENO," *Proc. Int. Conf. Physics of Reactors—Nuclear Power: A Sustainable Resource (PHYSOR'08)*, Interlaken, Switzerland, September 14–19, 2008.

11. "International Handbook of Evaluated Criticality Safety Benchmark Experiments," NEA/NSC/DOC(95)03, Organisation for Economic Co-operation and Development (Sep. 2009).